Ionization Potential Depression Model for Warm/Hot and Dense Plasmas

Chensheng Wu(武晨晟)[1,2†], Fuyang Zhou(周福阳)[1†], Jun Yan(颜君)[1], Xiang Gao(高翔)[1*], Yong Wu(吴勇)[1*], Chunhua Zeng(曾春华)[2], and Jianguo Wang(王建国)[1]

[1]*Institute of Applied Physics and Computational Mathematics, Beijing 100088, China*
[2]*Faculty of Science, Kunming University of Science and Technology, Kunming 650500, China*

(Received 27 May 2024; accepted manuscript online 19 July 2024)

For warm/hot and dense plasmas (WDPs), ionization potential depression (IPD) plays a crucial role in determining its ionization balance and understanding the resultant microscopic plasma properties. A sophisticated and unified IPD model is necessary to resolve those existing discrepancies between theoretical and experimental results. However, the applicability of those widely used IPD models nowadays is limited, especially for the nonlocal thermodynamic equilibrium (non-LTE) dense plasma produced by short-pulse laser. In this work, we propose an IPD model that considers inelastic atomic processes, in which three-body recombination and collision ionization processes are found to play a crucial role in determining the electron distribution and IPD for a WDP. This IPD model is validated by reproducing latest experimental results of Al plasmas with a wide-range condition of 70 eV–700 eV temperature and 0.2–3 times solid density, as well as a typical non-LTE system of hollow Al ions. It is demonstrated that the present IPD model has a significant temperature dependence due to the consideration of the inelastic collision processes. With a lower computational cost and wider application range of plasma conditions, the proposed model is expected to provide a promising tool to study the ionization balance and the atomic processes, as well as the related radiation and particle transports properties of the WDP.

DOI: 10.1088/0256-307X/41/8/085202

Warm/hot and dense plasmas (WDPs) widely exist in stars and giant planets in the universe,[1,2] and recently can be created in laboratory experiments with high power lasers[3–6] and Z-pinches.[7–10] For atoms embedded in WDPs, their structures and properties will be significantly altered due to the complicated many-body interactions with the surrounding plasmas.[11–20] Ionization potential depression (IPD) is one of the most important parameters for atoms in a dense plasma, it can significantly influences the ionization balance[21,22] and further impact the corresponding optical and thermodynamic properties of the plasma.[23,24] Especially, in the latest experiment in National Ignition Facility (NIF), successful ignition has been achieved,[25] which has once again gained widespread attention from the scientific community, bringing inertial confinement fusion (ICF) into the spotlight. Nevertheless, an accurate plasma simulation and diagnosis, which is highly sensitive to the ionization balance, is essential for the research of ICF. As such, a reliable IPD model is highly required.[26–29]

Recent laboratory advances in creating uniform and well-characterized high-energy-density plasmas allow for precise measurements of energy level shifts and IPD of dense plasmas.[3–5,30,31] The measured data, however, do not agree with the predictions of those widely used analytical IPD models, including Stewart–Pyatt (SP)[3,5,32] and Ecker–Kröll (EK)[4,33] models. The results from the experiments at the Linac Coherent Light Source (LCLS) favor the earlier EK model,[3,5] whereas the later experimental results of the ORION laser system, which created plasmas with higher densities and temperatures than LCLS, are better explained by the SP model.[4] Up to date, the underlying reason for the discrepancies of the EK and SP models under different plasma conditions remains unclear and has induced extensive theoretical investigations, including the two-step average atom model,[34] ion-sphere models,[22] fundamental plasma calculations,[35,36] classical molecular dynamics,[37] Monte Carlo simulations,[38] quantum statistical theory,[39] and *ab initio* calculations based on the density functional theory.[40,41] However, most of these theoretical studies are restricted with large computational cost or application with limited plasma conditions, mainly focusing on zero temperature[40,41] and under the local thermodynamic equilibrium (LTE) conditions.[22,34–36,38–41] Recently, a Monte Carlo molecular dynamics (MD) method was developed by Jin *et al.* to study the transient IPD evolution under non-LTE conditions, which only considers the screening effects of classical free electrons.[42] For those plasmas produced by short-pulse laser, the distribution of high-energy part of free electrons can reach equilibrium rapidly due to the large reaction rates of electron–electron and electron–ion elastic collision (EC) processes. However, the low-energy part of electron distribution is strongly influenced by inelastic

†These authors contributed equally to this work.
*Corresponding author. Email: gao_xiang@iapcm.ac.cn; wu_yong@iapcm.ac.cn
© 2024 Chinese Physical Society and IOP Publishing Ltd

collision processes between electrons and ions, which cause the electron distribution deviates from LTE conditions and those popular LTE models do not work further. Thus, it is crucial to construct a unified model to consider the non-LTE electron distribution effects in modeling IPD, and it is expected to unveil the fundamental microscopic mechanism of the discrepancies of the EK and SP models.

In this Letter, we propose an IPD model that considers the non-LTE electron distribution due to the contributions of collision processes in a unified framework. The feasibility and validation of the model are demonstrated by well reproducing the recent experimental IPD results with wide temperature and density ranges. Moreover, excellent agreements are also achieved for highly excited hollow Al ions between the present model predictions and the latest experiments, in which the IPD results are found to be highly sensitive to the related specific atomic processes for such a non-LTE system.

In a plasma environment, the distribution of plasma electrons effectively screens Coulomb interactions between the nucleus and bound electrons, significantly affecting the IPD. The first-order perturbation expression of the IPD can be written as

$$\Delta I = \langle \Psi | V_{\rm scr} - V_{\rm iso} | \Psi \rangle - V_{\rm scr}(Q,\, r_{\rm s}), \tag{1}$$

where $|\Psi\rangle$ is the atomic orbital function (AOF) of bound electron, $V_{\rm iso}$ is the effective potential felt by an isolated ion, $V_{\rm scr}$ is the screened potential felt by the target ions embedded in plasma and can be obtained by

$$V_{\rm scr}(Q,\, \boldsymbol{r}) = -\frac{Z}{r} + \int \frac{\rho_{\rm b} + \delta\rho(\boldsymbol{r'})}{|\boldsymbol{r} - \boldsymbol{r'}|} d\boldsymbol{r'}. \tag{2}$$

Here, Z is the nuclear charge number, Q is the ionization degree, $\delta\rho(\boldsymbol{r})$ is the plasma electron density fluctuation induced by the presence of the target ion, $\rho_{\rm b}$ is the density distribution of bound electrons of the target ion and can be calculated by using the occupation number and the AOF of bound electrons.[43] In Eq. (1), the contribution of electron screening on IPD is described by the difference between $V_{\rm scr}$ and $V_{\rm iso}$, and the electron can be ionized in plasma when its energy becomes higher than $V_{\rm scr}(r_{\rm s})$ with $r_{\rm s} = (3Q/4\pi\rho_0)^{1/3}$ being the Wigner–Seitz radius.[34] Therefore, the key issues of IPD calculation are the screened potential $V_{\rm scr}$ and the plasma electron density fluctuation $\delta\rho(\boldsymbol{r})$.

The EK, SP, and several other LTE theoretical models only consider free electrons with a total energy $E > 0$, considering only the contribution of EC processes. Nonetheless, plasma electrons can temporarily recombine with ions, and distribute into negative-energy states with $E < 0$ through three-body recombination (TBR), dielectronic recombination (DR), and radiative recombination (RR) processes. Consequently, the plasma electron density fluctuation can be expressed as

$$\delta\rho(\boldsymbol{r}) = \frac{1}{\pi^2}\left[\int_{\varepsilon_0}^{-V_{\rm scr}(Q,\,\boldsymbol{r})} f(\varepsilon,\, \boldsymbol{r})\varepsilon^{1/2} d\varepsilon + \int_{-V_{\rm scr}(Q,\,\boldsymbol{r})}^{\infty} f_{\rm FD}(\varepsilon,\, \boldsymbol{r})\varepsilon^{1/2} d\varepsilon\right] - \rho_0. \tag{3}$$

Here, ρ_0 is the mean electron density, $f_{\rm FD} = 1/\{\exp[(\varepsilon + V_{\rm scr} - \mu)/T_{\rm e}] + 1\}$ is the Fermi–Dirac distribution with chemical potential μ and the temperature of plasma electrons $T_{\rm e}$; ε is the kinetic energy of electrons and ε_0 is the lower limit of ε since the negative-energy electron prefers to populate the outer orbital unoccupied. In the dense plasma produced by short-pulse laser, the distributions of free electrons with a total energy $E = \varepsilon + V_{\rm scr}(\boldsymbol{r}) > 0$ are assumed to be in equilibrium and can be described by $f_{\rm FD}$, due to the large rates of electron–electron and electron–ion EC processes. However, since the rates of inelastic collisions between the electrons and ions are much lower, the distribution of negative-energy electrons with $E = \varepsilon + V_{\rm scr}(\boldsymbol{r}) < 0$ may not reach equilibrium during the pulse duration of laser. Theoretically, non-LTE distribution of negative-energy electrons $f(\varepsilon,\, \boldsymbol{r})$ should be calculated by solving the rate equations including all inelastic collision processes of the relevant ions with different charge states. Nevertheless, the time scales of TBR processes are around 10 fs due to the larger collision rates in the laser-produced dense plasmas considered here, since the TBR rates are proportional to ρ_0^2. For the plasma produced by a short-pulse x-ray free electron laser in about 150 fs duration, the contributions of TBR processes on the negative-energy electron distribution should be non-negligible and the plasma electrons can reach a quasi-steady state through these rapid inelastic collision processes,[44] the contribution of TBR processes can be approximated analytically as

$$f_{\rm TBR}(\varepsilon,\, \boldsymbol{r}) = 2\sqrt{\frac{E_{\rm r}}{\pi T_{\rm e}}}\frac{e^{-E_{\rm r}/T_{\rm e}}}{\mathrm{erf}(\sqrt{E_{\rm r}/T_{\rm e}})} f_{\rm FD}(\varepsilon,\, \boldsymbol{r}). \tag{4}$$

Dependent only on the distribution of free electrons and the state of recombined ions, the complicated calculations of rate equations can be simplified greatly. Here, $E_{\rm r} = |\varepsilon + V_{\rm scr}(Q,\, \boldsymbol{r})|$ represents the absolute value of the total energy, and $\mathrm{erf}(x)$ is the error function. As shown in Fig. S1 and Table S1 in the Supplementary Material, TBR processes dominate the distribution of negative-energy electrons in the WDP due to the larger collision rates. Thus the contributions from other inelastic collision processes to IPD can be evaluated using the first-order perturbation approximation by comparing their rates with TBR:

$$\eta_P = \frac{R_P^{Q+} N_P^{Q+}}{R_{\rm TBR}^{q+} N_{\rm TBR}^{q+}}, \tag{5}$$

where R_P^{Q+} and N_P^{Q+} are the rate coefficients and the populations of the initial state ions of inelastic collision processes P, $R_{\rm TBR}^{q+}$ and $N_{\rm TBR}^{q+}$ are the ones of TBR process. The negative-energy electron distribution $f(\varepsilon,\, \boldsymbol{r})$ can be calculated with $f = f_{\rm TBR} + \sum_P f_P$, in which the contribution of a specific process P is $f_P = \eta_P f_{\rm TBR}$. Then, the contributions from different collision processes can be included approximately in a unified framework. The IPD of ions in different charge states can be calculated using Eqs. (1)–(5) through an iterative approach. The numerical costs are dependent on the desired precision. In the

present calculation, we can take a few minutes to obtain the IPDs for a particular ionization degree using a single thread on a personal computer. The detail of the numerical method can be found in the Supplementary Material.

It should be mentioned that to finalize the calculation, it is essential to determine the AOF $|\Psi\rangle$ and rate coefficients in the corresponding charge states. However, both the AOF and rate coefficients are influenced by the plasma, and accurately calculating of these parameters in dense plasma is another challenging problem, which is beyond the scope of this work. The primary objective of our current work is to establish a foundational framework that incorporates non-LTE effects in plasma research. Note that the influence of plasma screening on the AOF we used is limited under the discussed plasma conditions, we derived the AOF using the multi-configuration Dirac–Fock (MCDF) method without considering plasma screening.[43] Additionally, we employed a set of semi-empirical formulas to facilitate the calculation of rate coefficients, with plasma influences accounted for by adjusting ionization thresholds and transition energies in these formulas based on IPD. Improving the model with more precise rates of microscopic atomic processes is undoubtedly a focal point of our future research.

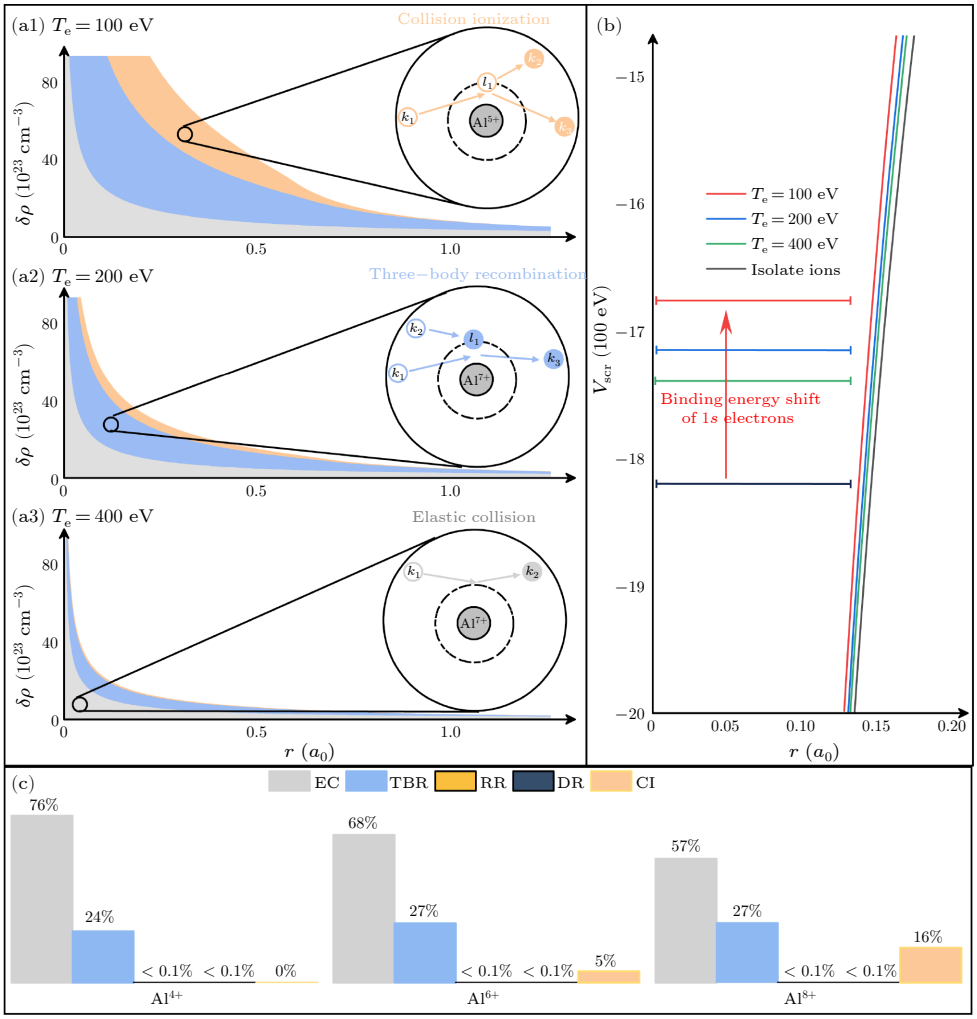

Fig. 1. (a1)–(a3) The contribution from different inelastic collision processes to the plasma electron density fluctuation of Al^{7+} in solid density and T_e = 100, 200, 400 eV, respectively. (b) The screened potentials and binding energies of 1s electrons of Al^{7+} embedded in the related plasmas. (c) The contribution of different collision processes to the IPD in solid density Al plasma with T_e = 85 eV. EC: elastic collision, TBR: three-body recombination, RR: radiative recombination, DR: dielectronic recombination, CI: collisional ionization.

The present model is first applied to address the issue of IPD in the recent LCLS experiments,[3,5] in which the density of ions ρ_i is similar to those in solid materials and electron temperature T_e ranges from 70 eV to 180 eV.[3] As discussed above, the target ion A^{q+} can temporarily combine with a negative-energy electron to form $A^{*(q-1)+}$ through TBR, RR, and DR processes. Additionally, $A^{*(q-1)+}$ can be generated through the electron–ion collision ionization (CI) processes of $A^{(q-2)+}$. The rate coefficients for these inelastic processes and their contributions to IPD can be calculated using the approach presented in the Supplementary Material. As shown in

Fig. 1(a), inelastic collision processes significantly affect the WDP electron distribution. Furthermore, the contribution of elastic and inelastic processes to IPD in Al^{4+}, Al^{6+} and Al^{8+} with solid density and $T_e = 85$ eV is calculated and depicted in Fig. 1(c). It is observed that the contribution of TBR and CI processes to IPD is critical in these cases, particularly for ions in high charge states, while the contributions of DR and RR processes are significantly smaller. Therefore, in addition to EC processes, TBR, and CI processes should be considered in the IPD modeling in WDP.

The proposed model is validated by calculating IPD of Mg and Al ions with different charge states at $T_e = 70$, 85, 100 eV and ρ_i at solid material density, which is consistent with the experimental conditions. For comparison, IPD calculated by SP and EK models are also presented. As shown in Figs. 2(a) and 2(b), the present IPD results ΔI are in good agreement with the experimental values. In similarity with previous LTE models, the results ΔI_0 of elastic collision (EC) model are calculated without including the contribution from inelastic collision processes, and found to significantly underestimate the IPDs. Therefore, it can be concluded that the inclusion of inelastic collision processes is necessary to accurately modeling the IPDs in WDP.

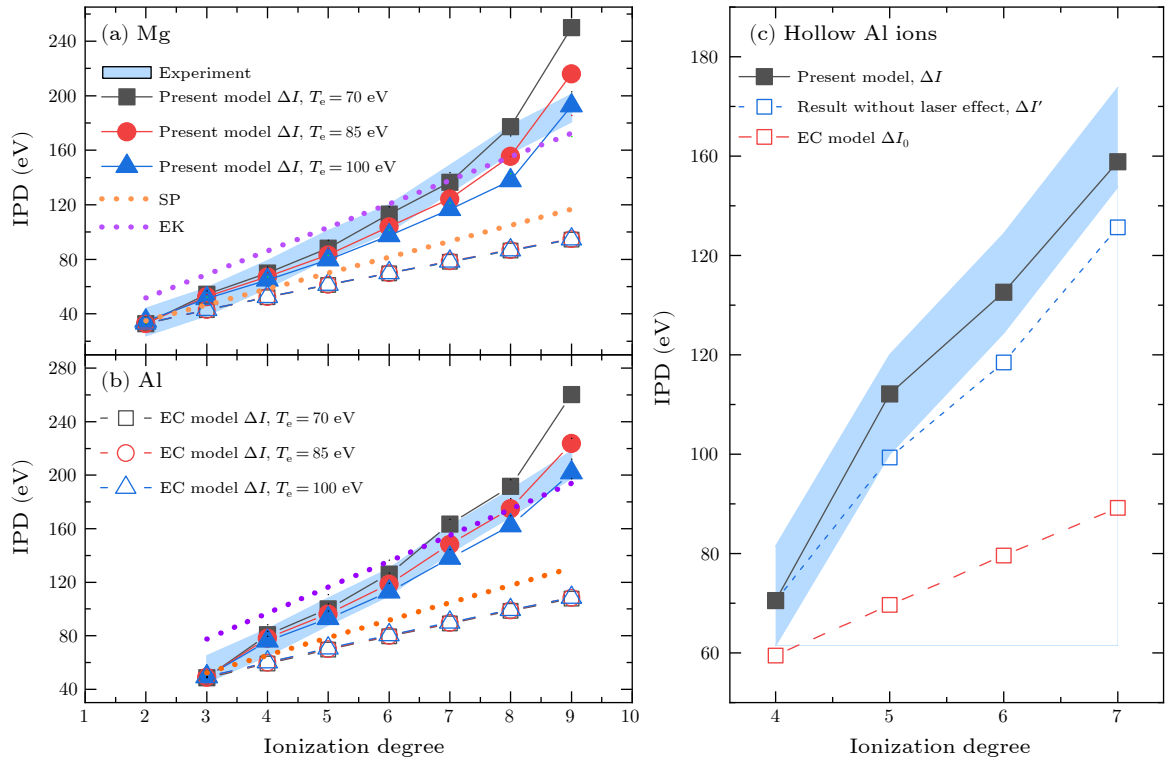

Fig. 2. The IPD calculated in the present model and the comparison with the LCLS experiment.[5] [(a), (b)] The IPD of Mg and Al ions with solid density and $T_e = 70$, 85 and 100 eV. ΔI represents the results of the present model, and ΔI_0 shows the results of the EC model that has excluded the contribution from inelastic collision processes. (c) The IPD of hollow Al ions with solid density and $T_e = 70$ eV. For such a non-LTE system, the results are sensitive to the specific atomic processes, and the results $\Delta I'$ without considering the impact of the pump laser on IPD are also presented.

In detail of Fig. 2(a), the IPDs of Mg ions with $T_e = 70$ eV are in good agreement with the experimental data for most of the ionization degrees, except for Mg^{9+} where the calculations show higher values. However, when higher temperatures ($T_e = 85$, 100 eV) are applied, a good agreement between calculations and experiments is achieved for Mg^{9+}. The same trend is also observed for Al ions. The discrepancies observed at high ionization degrees between our calculations and experiments may arise from an underestimation of the plasma temperature. In experiments, higher ionization degrees require higher pump photon energies, which in turn assume higher temperatures for ions with higher ionization degree.[3,5] By introducing a higher temperature, the theoretical results become consistent with the experimental data. Note that, without considering the contribution of inelastic collision processes, the calculated IPDs ΔI_0 are almost the same for different temperatures. In contrast, a stronger temperature dependence in the present model is induced by taking into account the inelastic collision processes that are highly sensitive to the temperature and density of the plasma.

Furthermore, the current non-LTE IPD model is applied to calculate the IPD of $1s$ hollow Al ions, which were detected in the LCLS experiment.[3] Here $1s$ hollow Al ions decay rapidly through radiative transitions and Auger processes, and thus their lifetimes are only 2 fs–3 fs, which is

even smaller than the plasma equilibrium time and the timescale of the inelastic collision processes. As a result, the relaxation of plasma electron distributions should be neglected during the short lifetime of these ions. Instead, the plasma electron distributions surrounding the hollow ions can be obtained from the ones before the ionization of $1s$ electron. However, for this non-LTE system, the impact of the pump laser on the IPD is significant. In the experiment, the $1s$ hollow Al ions are generated by pump laser photoionization. The pump laser's selection effect on negative-energy electron distributions must be taken into account since the photoionization cross sections differ between ions with and without negative-energy electrons. Accounting for this impact, the proportion of hollow ions with and without negative-energy electrons can be expressed as

$$\frac{N_{1s}^{*(q-1)+}}{N_{1s}^{q+}} = \frac{N^{*(q-2)+}\sigma^{*(q-2)+}(\omega)}{N^{(q-1)+}\sigma^{(q-1)+}(\omega)}, \tag{6}$$

where $N_{1s}^{*(q-1)+}$ and N_{1s}^{q+} are the populations of $1s$ hollow ions with and without combining negative-energy electron, respectively; ω is the photon energy of pump laser; $\sigma^{*(q-2)+}(\omega)$ and $\sigma^{(q-1)+}(\omega)$ are the photoionization cross sections of the related ground-state ions $A^{*(q-2)+}$ and $A^{(q-1)+}$, respectively. $N^{*(q-2)+}$ and $N^{(q-1)+}$ are the populations of related ground-state ions. Then the distribution of negative-energy electrons in $1s$ hollow ions $f^{1s}(\varepsilon, \boldsymbol{r})$ can be expressed as $f^{1s} = \eta_\sigma f$ with $\eta_\sigma(\omega) = \sigma^{*(q-2)+}(\omega)/\sigma^{(q-1)+}(\omega)$.

Based on the above treatments, the IPDs of $1s$ hollow Al ions are calculated with solid density and $T_e = 70\,\text{eV}$ and compared with the experiment in Fig. 2(c). The uncertainty of measurements is given as 10 eV, which is estimated by the IPD of unionized ions in Ref. [3]. The present results ΔI are in great agreement with the experimental measurements, further verifying the reliability of the present model on such a non-LTE system. For comparison, the results of the EC model ΔI_0 are presented and are found to significantly underestimate the IPD of hollow Al ions, elucidating the importance of inelastic collision processes. Furthermore, the results $\Delta I'$ without the consideration of the selection effect of the pump laser are also presented in Fig. 2(c), and are found to underestimate the IPD. This indicates that the non-LTE electron distribution is sensitive to the specific atomic processes, and an insufficient consideration of the corresponding atomic processes would lead to an evident discrepancy in the prediction of non-LTE IPD.

To gain deeper insight into the temperature dependence of IPD, Fig. 3 displays the IPD results of ground-state ions of Al^{7+}, Al^{9+}, and Al^{11+} versus temperature. Additionally, the results from widely used SP, EK, ion-sphere (IS) and Debye–Hückel (DH) models[45] and the data from the LCLS and Orion experiments[3–5] are presented for comparison. Figure 3 shows that the IPD results are close to the EK model and to the experiment under the plasma condition with $T_e \sim 100\,\text{eV}$ and electron density in $5 \times 10^{23}\,\text{cm}^{-3}$ corresponding to the LCLS experiment, while the SP model underestimates the IPD evidently.[3,5] For higher temperature and density when $T_e > 550\,\text{eV}$ and electron density in $1.5 \times 10^{24}\,\text{cm}^{-3}$ corresponding to the Orion experiment,[4] our results are evidently lower than the EK model and close to the SP model. Under this plasma condition, the EK model overestimates the IPD, and our model demonstrates better agreement with the experimental measurements.[4] For high temperature areas, the plasma electrons are dominated by free electrons as shown in Fig. 1, causing our model to converge to the SP model. In the middle temperature area with $250\,\text{eV} < T_e < 375\,\text{eV}$, the validity of our model is validated based on the measured $K\alpha$ line shift in Al^{11+}. This shift refers to the difference in binding energy shifts between $1s$ and $2p$ due to the plasma environment. Our previously published work[44] demonstrates excellent agreement between our model and experimental measurements, whereas the IS models underestimate the line shifts.[46] The present model exhibits a stronger temperature dependence and can effectively treat plasmas with wider ranges of temperatures and densities.

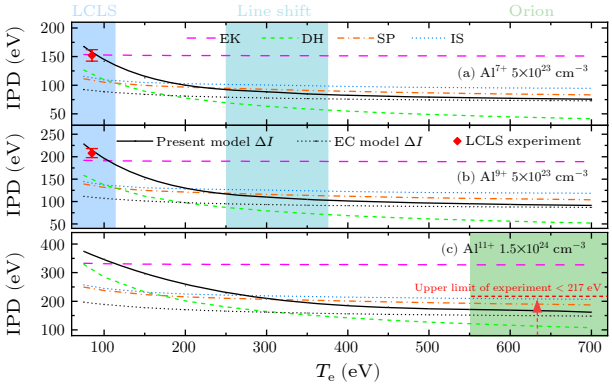

Fig. 3. The IPD of Al^{7+}, Al^{9+}, and Al^{11+} ions versus temperature (from 75 eV to 500 eV) at a fixed electron density of $5 \times 10^{23}\,\text{cm}^{-3}$ for Al^{7+} and Al^{9+}, and $1.5 \times 10^{24}\,\text{cm}^{-3}$ for Al^{11+}, respectively. ΔI represents the results of the present model, and ΔI_0 shows the results of the EC model without the contribution of inelastic collision processes. The results from other theoretical models and experiments are also shown for comparison.

For further illustration, we also computed the results in the EC model without accounting for inelastic collision processes, as presented in Fig. 3. Our results clearly demonstrate that accounting for inelastic collision processes results in a stronger temperature dependence. However, the SP model only considers the contribution of free electrons on the screening effect, so its temperature variation tendency is similar to our results of the EC model. Similarly, the EK model is only dependent on plasma density and has no explicit temperature dependence.[3] In a word, the SP and EK models fail to work in warm-dense plasmas and high temperature range, respectively, due to their inadequate description of temperature dependence.

In summary, we have proposed an IPD model for WDP, especially for the one produced by short-pulse laser, which

can account for the non-LTE effect due to the contributions of different inelastic collision processes. As non-LTE systems are sensitive to specific atomic processes, accurately modeling IPD requires taking these inelastic collision processes into account. Rather than directly solving the complicated rate equations that include all collision processes, the contributions of different inelastic collision processes on the electron distribution are approximately obtained based on the analytical form of contribution of TBR process, and thus the computational complexity of our model is nearly same as those of LTE models. The proposed model is successfully validated by well reproducing the IPD results of the recent WDP experiments. In particular, an excellent agreement is achieved in comparison with the IPD of hollow Al ions for the first time. Our results indicate that the inelastic collision processes, particularly TBR and CI processes, are important and should be accounted for accurately modeling the IPD in WDP. Furthermore, inclusion of the inelastic collision processes leads to a stronger temperature dependence of IPD in the present model, and we demonstrate that the inadequate consideration of the collision processes makes the SP and EK models only valid for plasma under specific temperature and density conditions. Our work provides a promising tool for treating IPD in a wide range of temperatures and densities, which will facilitate future studies of radiation and particle transport properties of WDP.

Acknowledgments. This work was supported by the National Key R&D Program of China (Grant No. 2022YFA1602500), the National Natural Science Foundation of China (Grant Nos. 12204057, 12241410, and 11734013), and the Yunnan Applied Basic Research Projects (Grant No. 202401CF070090). We acknowledge the computational support provided by the Institute for Applied Physics and Computational Mathematics.

References

[1] Tayler R J 1994 *The Stars: Their Structure and Evolution* (Cambridge: Cambridge University Press)
[2] Helled R, Anderson J D, Podolak M, and Schubert G 2011 *Astrophys. J.* **726** 15
[3] Ciricosta O, Vinko S M, Chung H K *et al.* 2012 *Phys. Rev. Lett.* **109** 065002
[4] Hoarty D J, Allan P, James S F *et al.* 2013 *Phys. Rev. Lett.* **110** 265003
[5] Ciricosta O, Vinko S M, Barbrel B *et al.* 2016 *Nat. Commun.* **7** 11713
[6] Vinko S M, Ciricosta O, Cho B I *et al.* 2012 *Nature* **482** 59
[7] Gomez M R, Slutz S A, Sefkow A B *et al.* 2014 *Phys. Rev. Lett.* **113** 155003
[8] Nagayama T, Bailey J E, Loisel G P *et al.* 2019 *Phys. Rev. Lett.* **122** 235001
[9] Hansen S B, Harding E C, Knapp P F, Gomez M R, Nagayama T, and Bailey J E 2017 *High Energy Density Phys.* **24** 39
[10] Bailey J E, Nagayama T, Loisel G P *et al.* 2015 *Nature* **517** 56
[11] Nguyen H, Koenig M, Benredjem D, Caby M, and Coulaud G 1986 *Phys. Rev. A* **33** 1279
[12] Chang T N, Fang T K, and Gao X 2015 *Phys. Rev. A* **91** 063422
[13] Janev R K, Zhang S B, and Wang J G 2016 *Matter Radiat. Extremes* **1** 237
[14] Fang T K, Wu C S, Gao X, and Chang T N 2017 *Phys. Rev. A* **96** 052502
[15] Fang T K, Wu C S, Gao X, and Chang T N 2018 *Phys. Plasmas* **25** 102116
[16] Wu C, Chen S, Chang T N, and Gao X 2019 *J. Phys. B* **52** 185004
[17] Ma Y, Liu L, Xie L, Wu Y, Qu Y, and Wang J 2020 *J. Quant. Spectrosc. Radiat. Transfer* **241** 106731
[18] Chang T N, Fang T K, Wu C S, and Gao X 2021 *Phys. Scripta* **96** 124012
[19] Chang T N and Gao X 2022 *Phys. Rev. A* **105** 056801
[20] Wu C S, Wu Y, Yan J, Chang T N, and Gao X 2022 *Phys. Rev. E* **105** 015206
[21] Mazzitelli G and Mattioli M 2002 *At. Data Nucl. Data Tables* **82** 313
[22] Zeng J, Li Y, Gao C, and Yuan J 2020 *Astron. Astrophys.* **634** A117
[23] Salzman D 1998 *Atomic Physics in Hot Plasmas* (New York: Oxfold University Press)
[24] Griem H R 1986 *Principles of Plasma Spectroscopy.* In: Thompson J E and Luessen L H (eds) *Fast Electrical and Optical Measurements. NATO ASI Series* (Dordrecht: Springer) vol 108/109 pp. 885–910
[25] Danson C N and Gizzi L A 2023 *High Power Laser Sci. Eng.* **11** e40
[26] Glenzer S H and Redmer R 2009 *Rev. Mod. Phys.* **81** 1625
[27] Nettelmann N, Redmer R, and Blaschke D 2008 *Phys. Part. Nucl.* **39** 1122
[28] Glenzer S H, MacGowan B J, Michel P *et al.* 2010 *Science* **327** 1228
[29] Fäustlin R R, Bornath T, Döppner T *et al.* 2010 *Phys. Rev. Lett.* **104** 125002
[30] Beiersdorfer P, Brown G V, McKelvey A, Shepherd R, Hoarty D J, Brown C R D, Hill M P, Hobbs L M R, James S F, Morton J, and Wilson L 2019 *Phys. Rev. A* **100** 012511
[31] Stillman C R, Nilson P M, Ivancic S T, Golovkin I E, Mileham C, Begishev I A, and Froula D H 2017 *Phys. Rev. E* **95** 063204
[32] Stewart J C and Jr Pyatt K D 1966 *Astrophys. J.* **144** 1203
[33] Ecker G and Kröll W 1963 *Phys. Fluids* **6** 62
[34] Son S K, Thiele R, Jurek Z, Ziaja B, and Santra R 2014 *Phys. Rev. X* **4** 031004
[35] Belkhiri M and Poirier M 2013 *High Energy Density Phys.* **9** 609
[36] Crowley B J B 2014 *High Energy Density Phys.* **13** 84
[37] Calisti A, Ferri S, and Talin B 2015 *J. Phys. B* **48** 224003
[38] Stransky M 2016 *Phys. Plasmas* **23** 012708
[39] Lin C 2019 *Phys. Plasmas* **26** 122707
[40] Vinko S M, Ciricosta O, and Wark J S 2014 *Nat. Commun.* **5** 3533
[41] Hu S X 2017 *Phys. Rev. Lett.* **119** 065001
[42] Jin R, Abdullah M M, Jurek Z, Santra R, and Son S K 2021 *Phys. Rev. E* **103** 023203
[43] Grant I P 2007 *Relativistic Quantum Theory of Atoms and Molecules* (New York: Springer Science+Business Media)
[44] Zhou F, Qu Y, Gao J, Ma Y, Wu Y, and Wang J 2021 *Commun. Phys.* **4** 148
[45] Debye P and Hückel E 1923 *Phys. Z.* **24** 185
[46] Chen Z B and Wang K 2020 *Radiat. Phys. Chem.* **172** 108816